

Supplementary Information

Synthesis and reactivity of Li and TaMe₃ complexes supported by *N,N'*-bis(2,6-diisopropylphenyl)-*o*-phenylenediamido ligands

Trevor Janes, Maotong Xu and Datong Song*

Davenport Chemical Research Laboratories, Department of Chemistry, University of Toronto

80 St. George Street, Toronto, Ontario, Canada M5S 3H6. Email: dsong@chem.utoronto.ca

Fax: + 1 416 978 7013; Tel: + 1 416 978 7014

Contents

1. NMR Spectra.....	S2
2. X-ray Crystallography.....	S14
3. EPR Spectroscopy	S19
4. References	S19

1. NMR Spectra

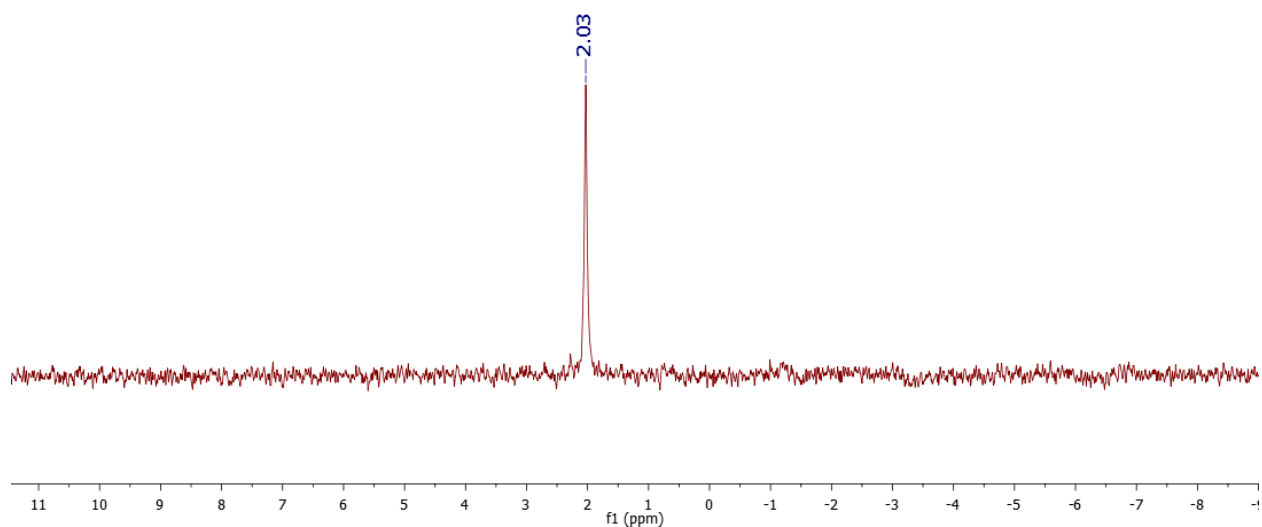


Figure S1. ^7Li NMR Spectrum (233 MHz, 25 °C) of **2** in C_6D_6

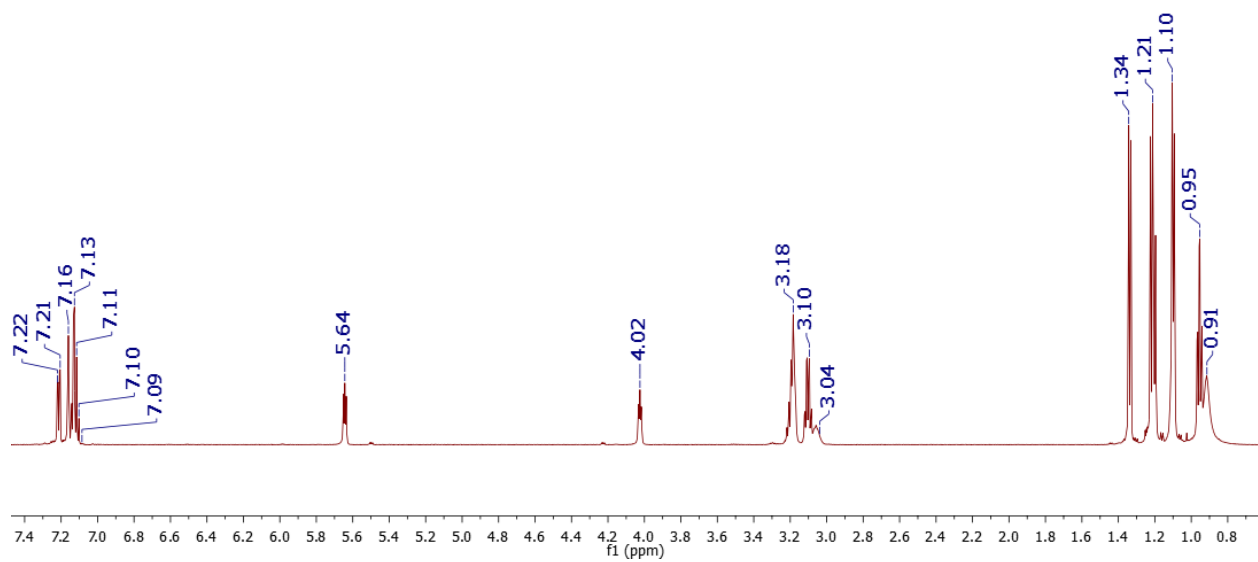


Figure S2. ^1H NMR Spectrum (600 MHz, 25 °C) of **2** in C_6D_6

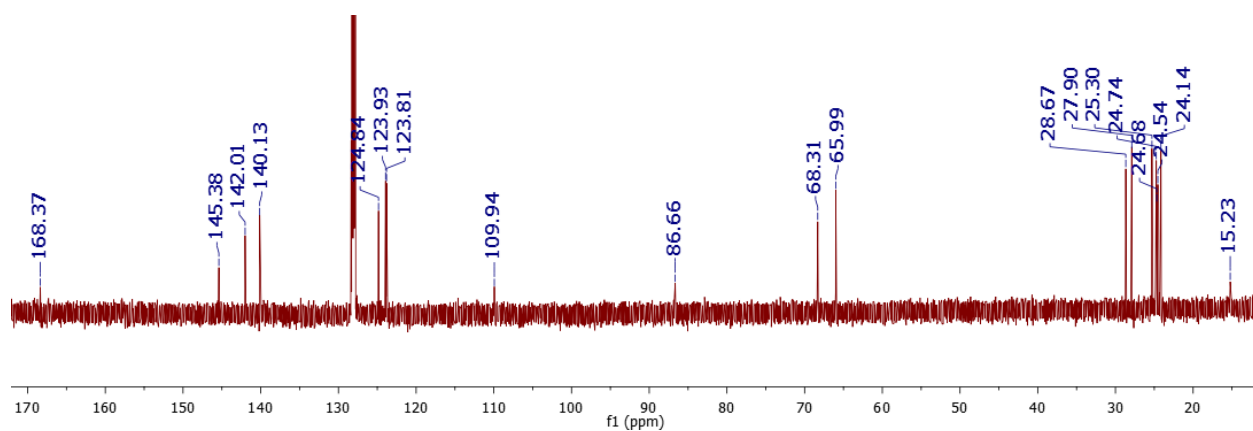


Figure S3. ^{13}C NMR Spectrum (151 MHz, 25 °C) of **2** in C_6D_6

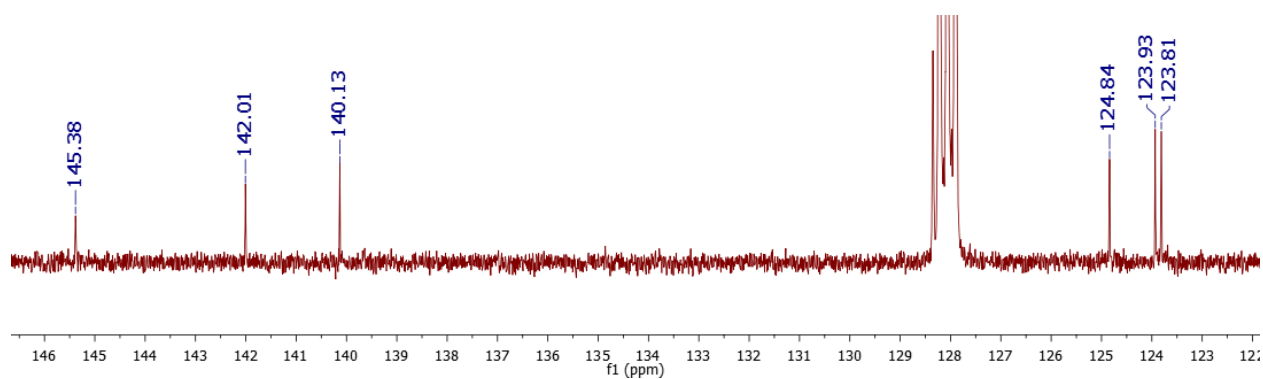


Figure S4. Aryl region of ^{13}C NMR Spectrum (151 MHz, 25 °C) of **2** in C_6D_6

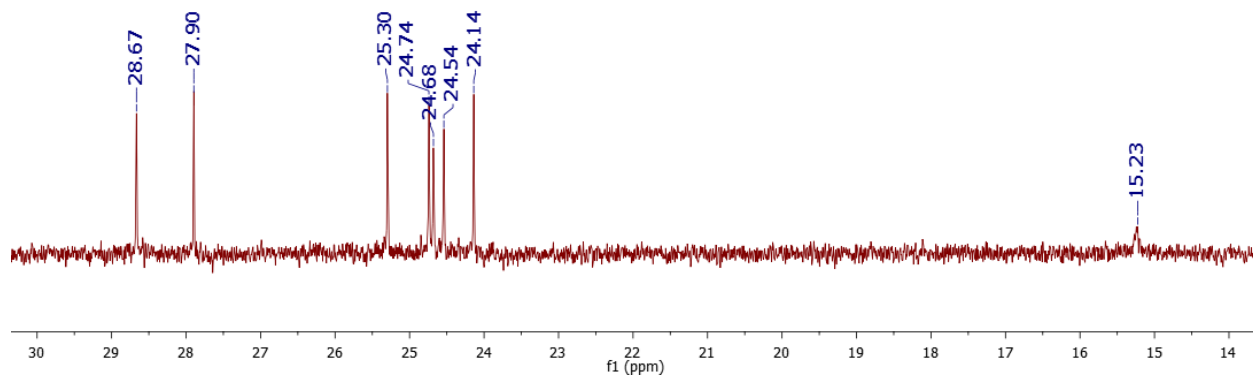


Figure S5. Alkyl region of ^{13}C NMR Spectrum (151 MHz, 25 °C) of **2** in C_6D_6

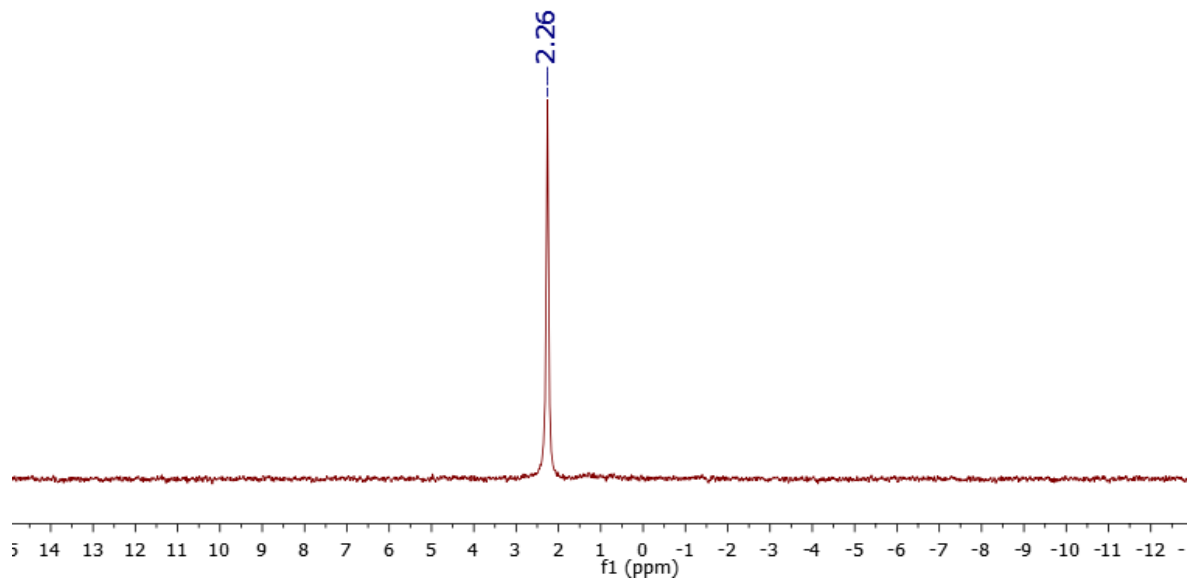


Figure S6. ^7Li NMR Spectrum (194 MHz, 25 °C) of **3**(thf) in C_6D_6

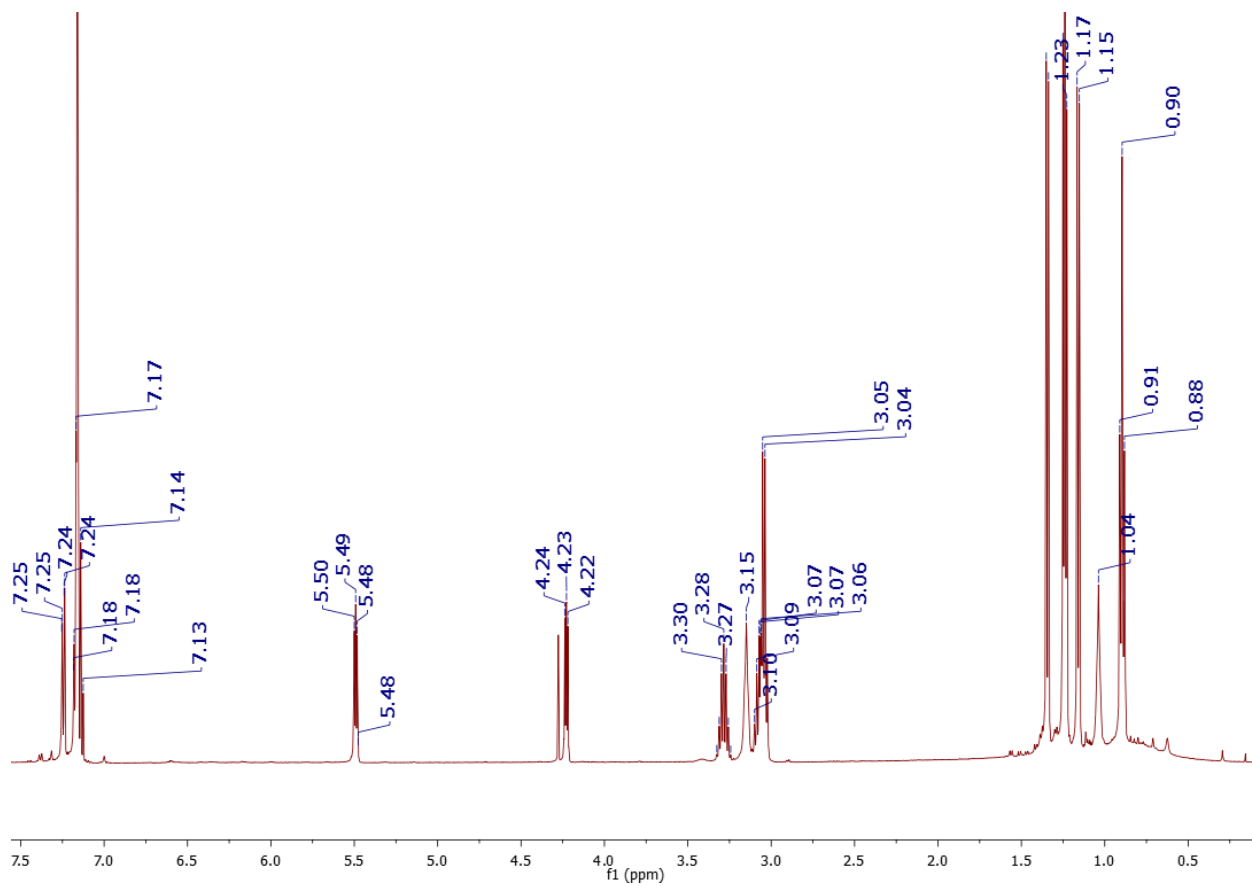


Figure S7. ^1H NMR Spectrum (500 MHz, 25 °C) of **3**(thf) in C_6D_6 . Note: spectrum contains dichloromethane at 4.28 ppm

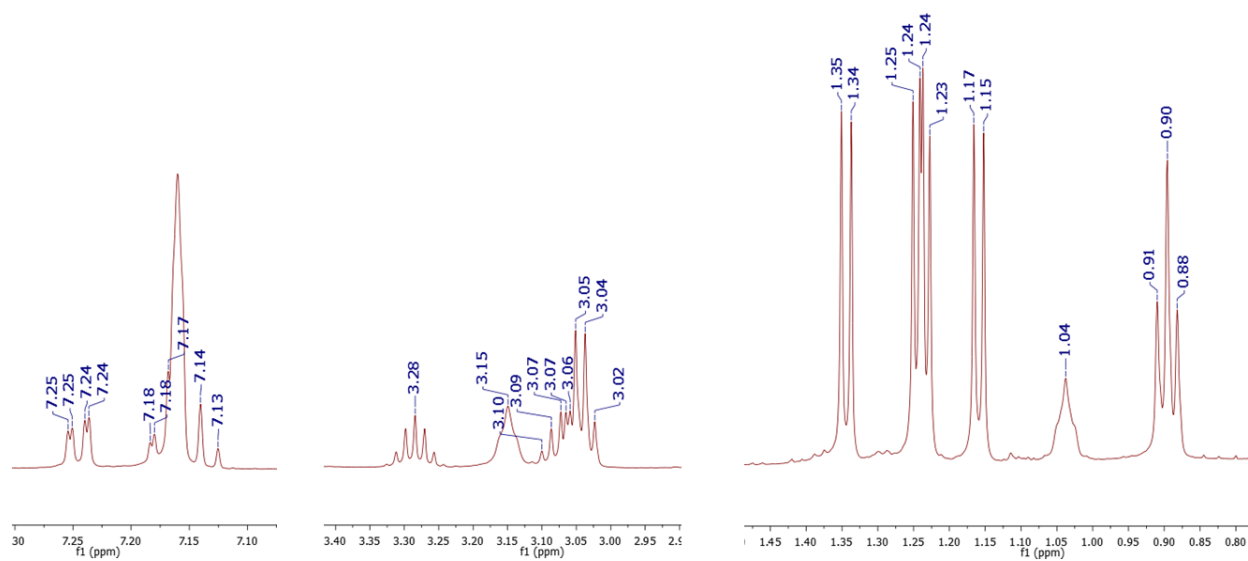


Figure S8. Expansion of selected regions of ^1H NMR Spectrum (500 MHz, 25 °C) of **3**(thf) in C_6D_6 .

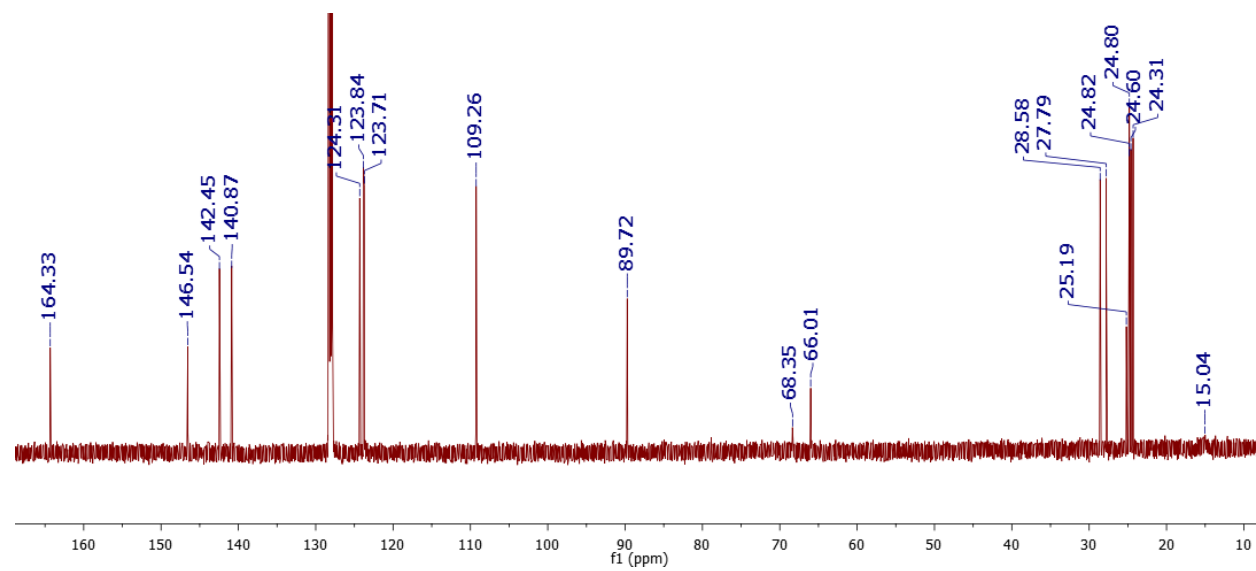


Figure S9. ^{13}C NMR Spectrum (126 MHz, 25 °C) of **3**(thf) in C_6D_6

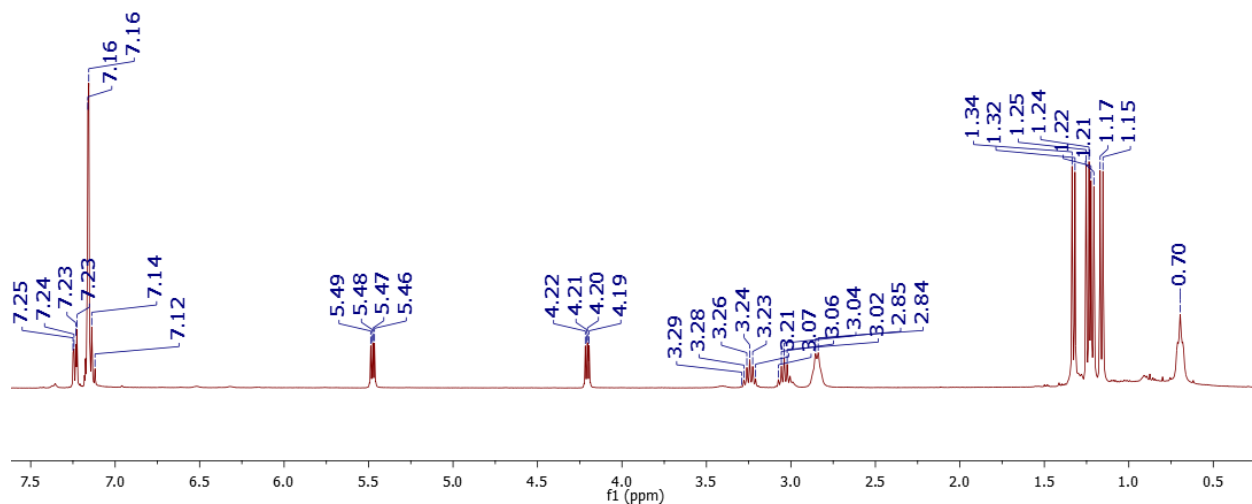


Figure S10. ^1H NMR Spectrum (400 MHz, 25 °C) of **3** in C_6D_6

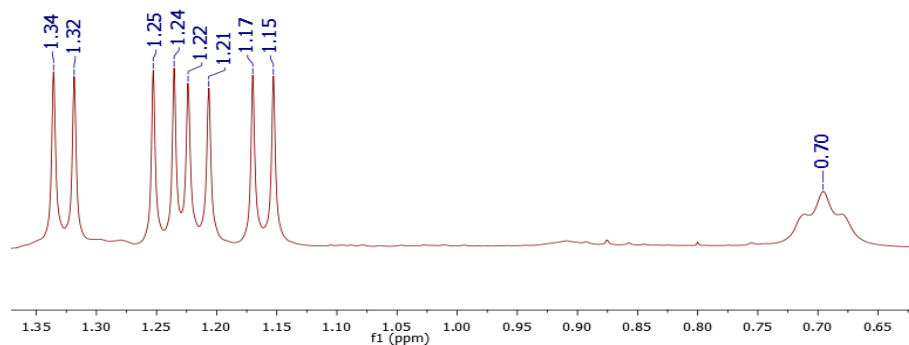


Figure S11. Expansion of the alkyl region of ^1H NMR Spectrum (400 MHz, 25 °C) of **3** in C_6D_6

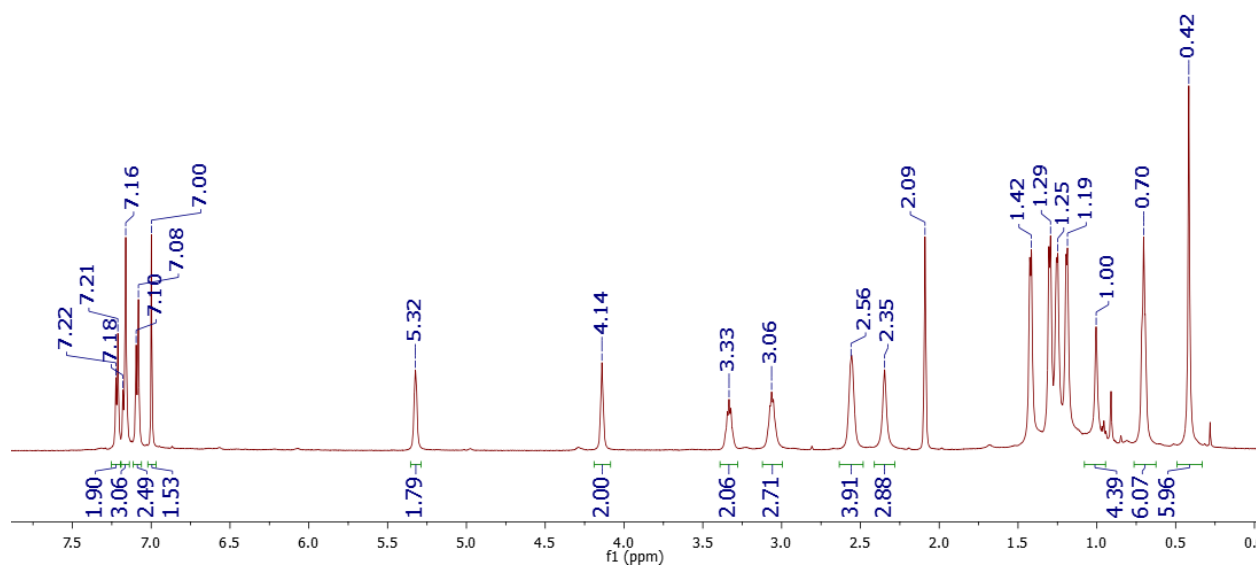


Figure S12. ^1H NMR Spectrum (600 MHz, -80 °C) of **3** in $\text{C}_6\text{D}_5\text{CD}_3$

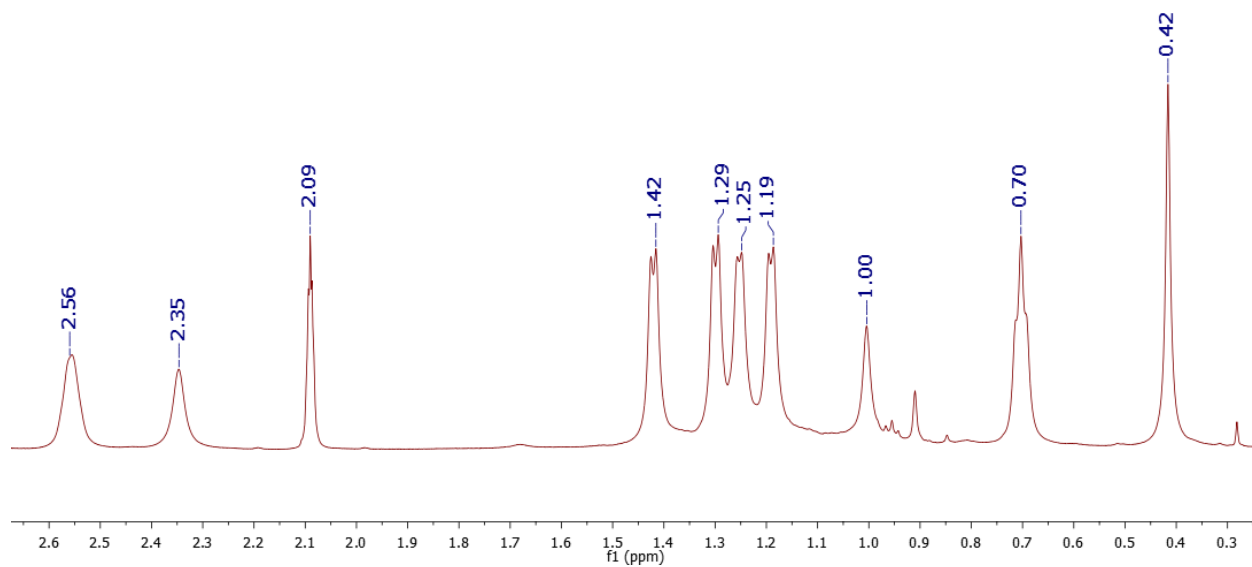


Figure S13. Expansion of the alkyl region of ^1H NMR Spectrum (600 MHz, 25 °C) of **3** in $\text{C}_6\text{D}_5\text{CD}_3$

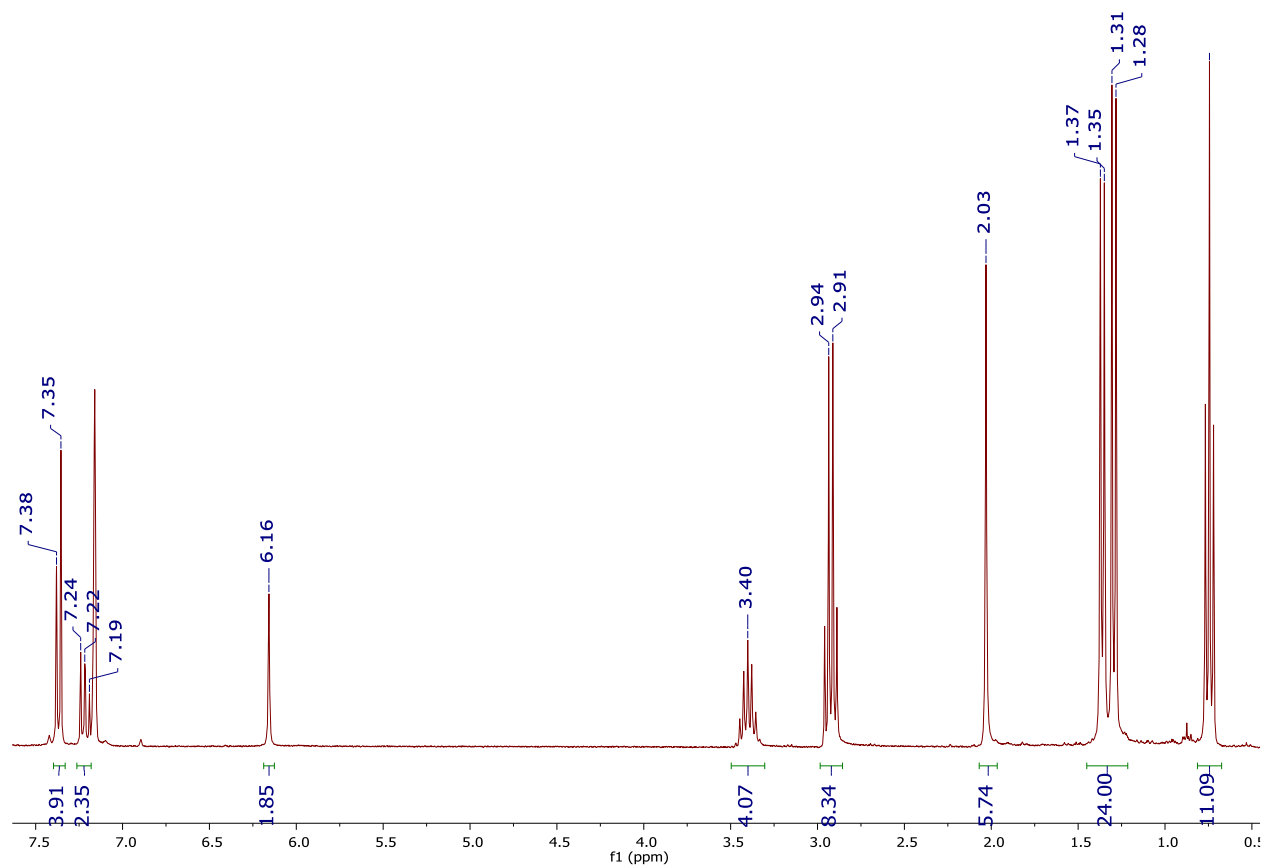


Figure S14. ^1H NMR Spectrum (300 MHz, 25 °C) of **5** in C_6D_6

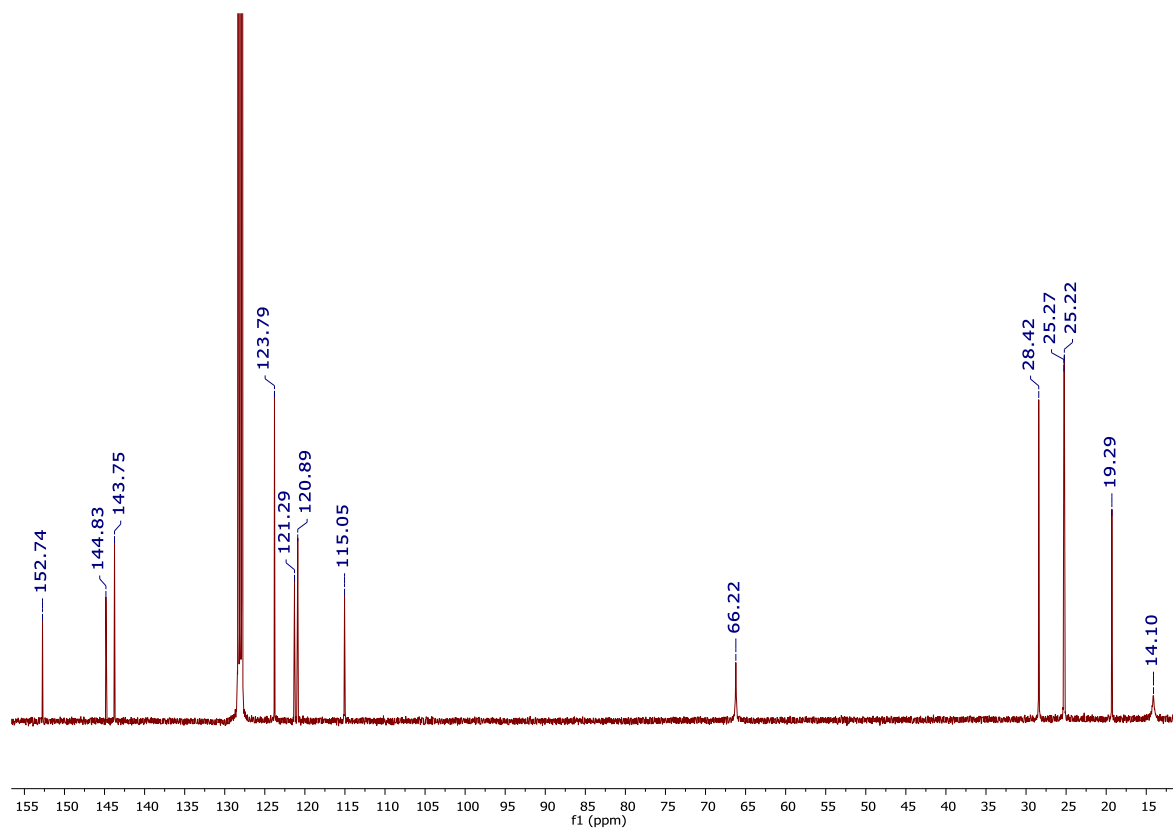


Figure S15. ¹³C NMR Spectrum (101 MHz, 25 °C) of **5** in C₆D₆

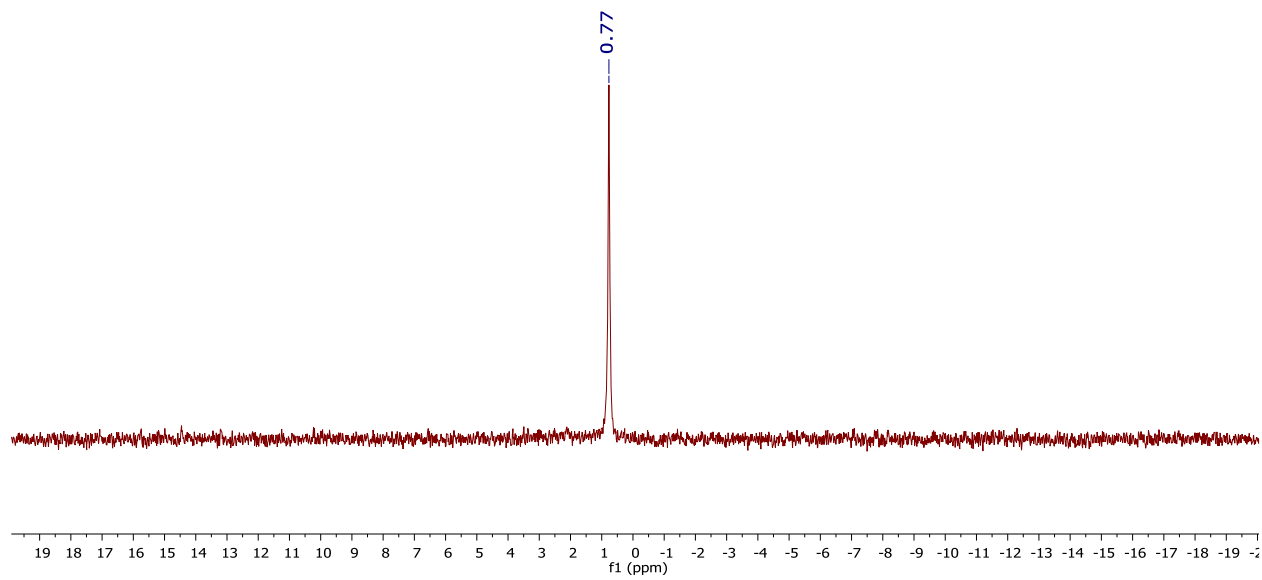


Figure S16. ⁷Li NMR Spectrum (194 MHz, 25 °C) of **5** in C₆D₆

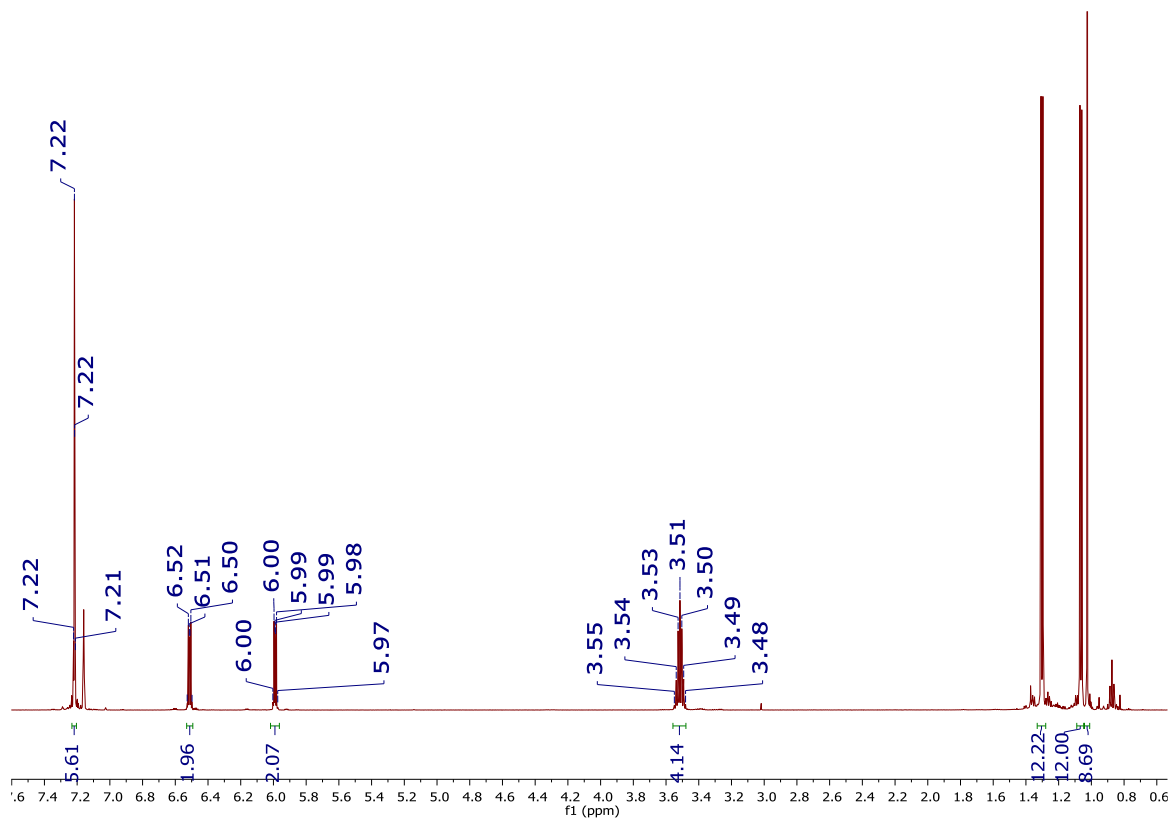


Figure S17. ^1H NMR Spectrum (600 MHz, 25 °C) of **8** in C_6D_6 spectrum contains pentane at 1.26 and 0.87

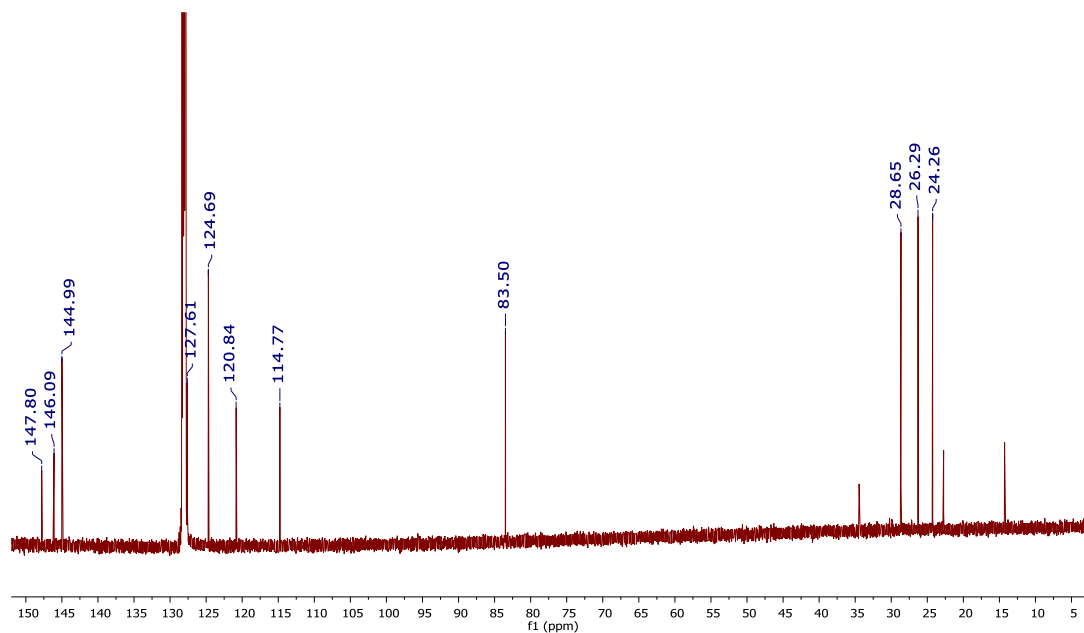


Figure S18. ^{13}C NMR Spectrum (151 MHz, 25 °C) of **8** in C_6D_6 Note: spectrum contains pentane at 34.45, 22.73, and 14.30.

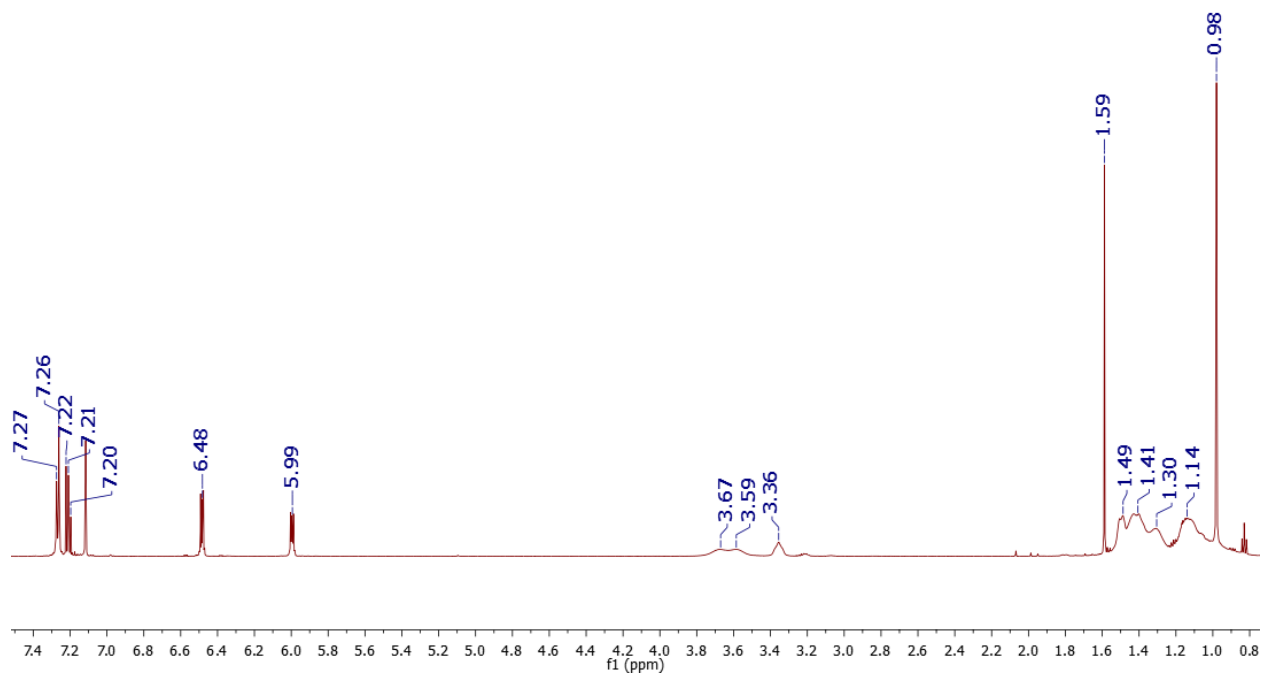


Figure S19. ^1H NMR Spectrum (600 MHz, 25 °C) of **9** in C_6D_6

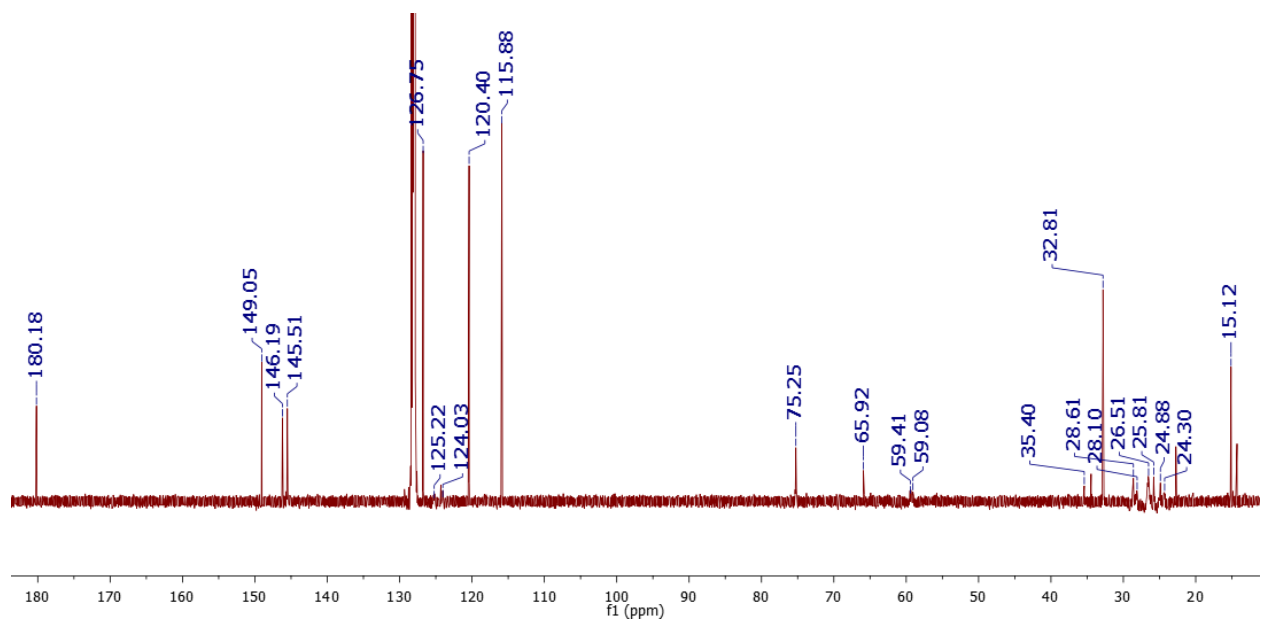


Figure S20. ^{13}C NMR Spectrum (151 MHz, 2 °C) of **9** in C_6D_6 .

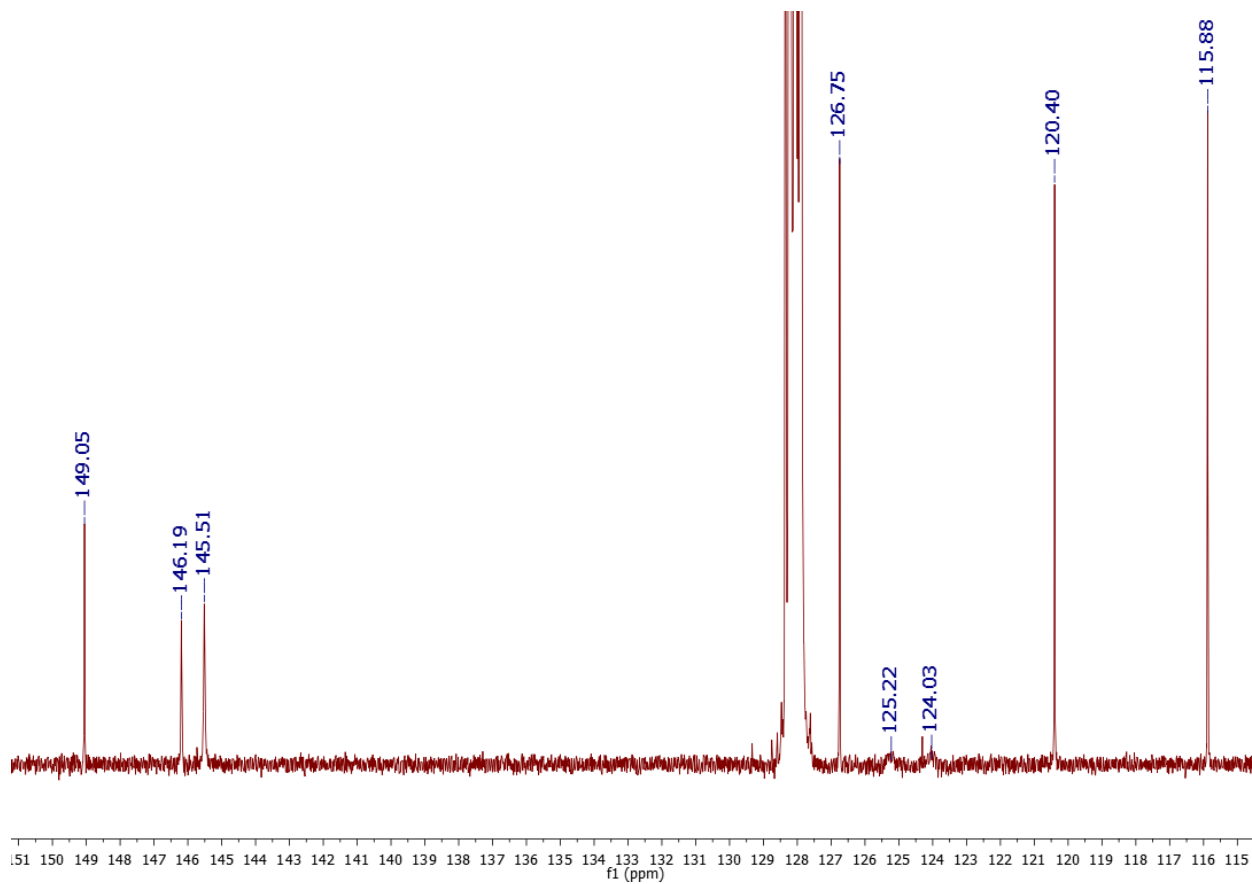


Figure S21. Aryl region of ^{13}C NMR Spectrum (151 MHz, 25 °C) of **9** in C_6D_6 .

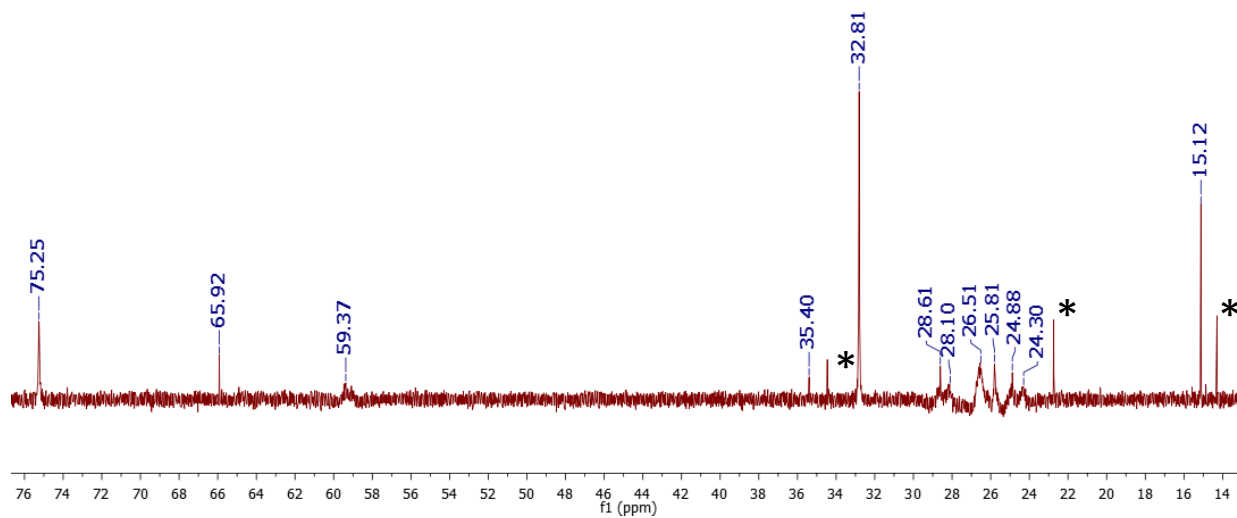


Figure S22. Alkyl region of ^{13}C NMR Spectrum (151 MHz, 25 °C) of **9** in C_6D_6 . Peaks due to residual pentane are marked with an asterisk.

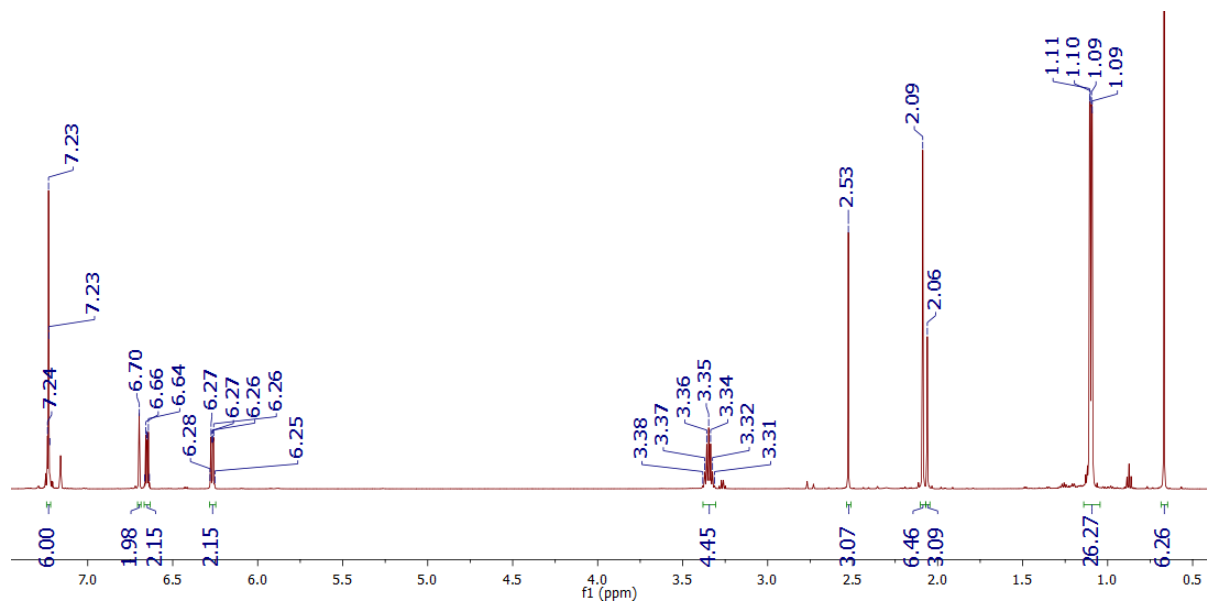


Figure S23. ^1H NMR Spectrum (600 MHz, 25 °C) of **10** in C_6D_6

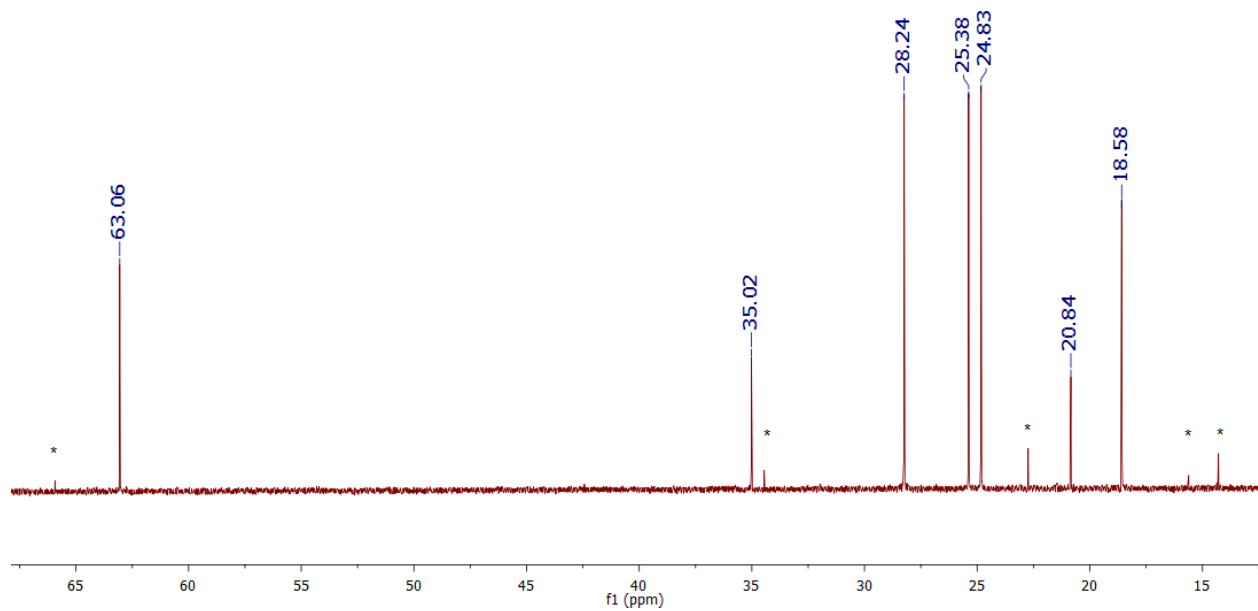


Figure S24. Alkyl region of ^{13}C NMR Spectrum (151 MHz, 25 °C) of **10** in C_6D_6 . Peaks due to residual pentane and Et_2O are marked with an asterisk.

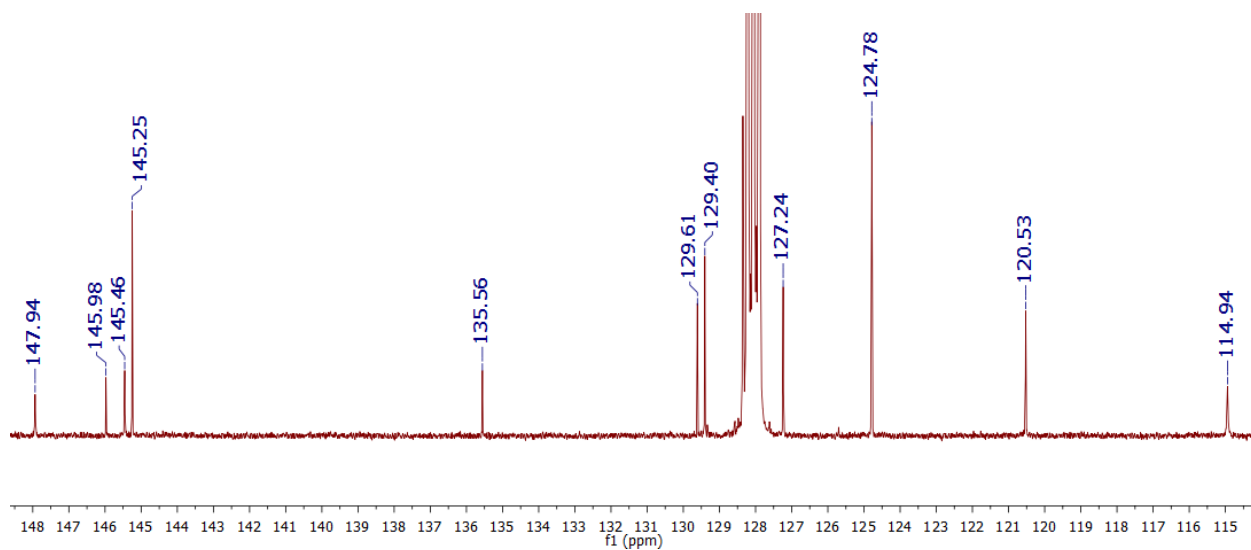


Figure S25. Aryl region of ^{13}C NMR Spectrum (151 MHz, 25 °C) of **10** in C_6D_6 .

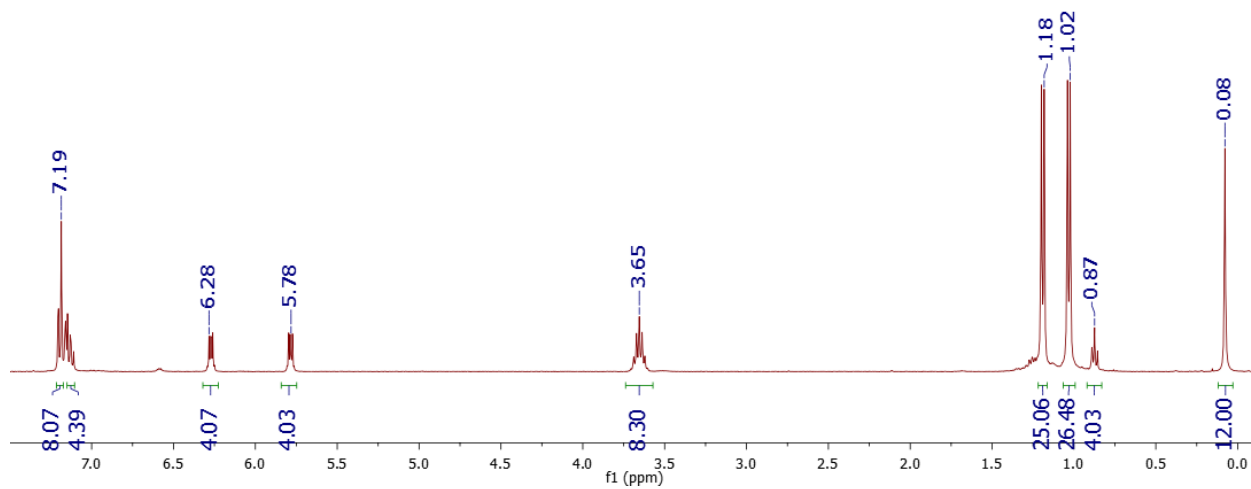


Figure S26. ^1H NMR Spectrum (400 MHz, 25 °C) of **11**(pentane) $_2/3$ in C_6D_6 .

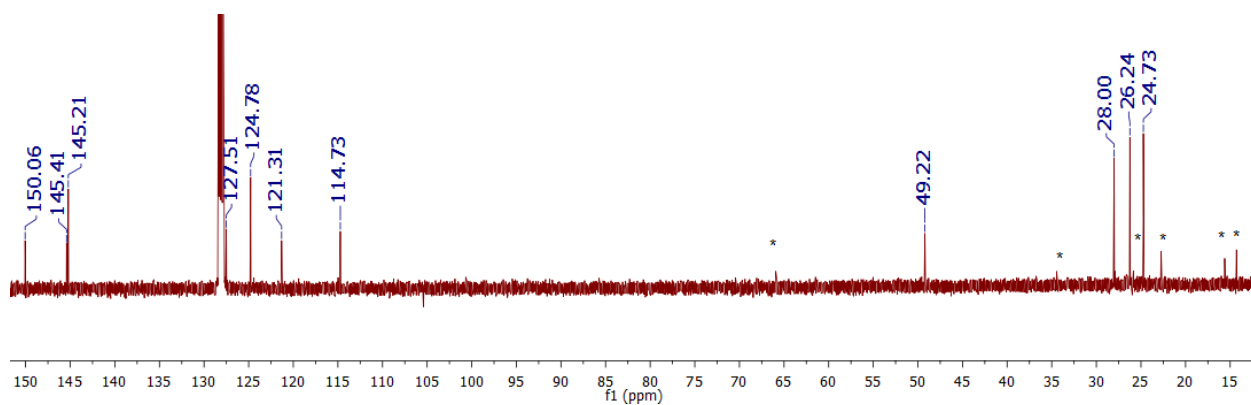


Figure S27. ^{13}C NMR Spectrum (500 MHz, 25 °C) of **11** in C_6D_6 Note: volatile impurities in the NMR solvent (THF, Et_2O , pentane) are marked with an asterisk

2. X-ray Crystallography

The X-ray diffraction data were collected on a Bruker Kappa Apex II diffractometer with graphite-monochromated Mo K α radiation ($\lambda = 0.71073 \text{ \AA}$) at 150 K controlled by an Oxford Cryostream 700 series low-temperature system and processed with the Bruker Apex 2 software package.¹ The structures were solved by direct methods and refined using SHELXL-2013 and SHELXL-2014.^{2,3} All non-hydrogen atoms were refined anisotropically, except for a few atoms involved in the disordered portions. All hydrogen atoms were calculated using the riding model. The diffuse residual electron density from a disordered cocrystallized pentane molecule in the lattice of **11** was removed with the SQUEEZE function of PLATON,⁴ and was not included in the formula or the refinement. Selected crystallographic data are listed in Table 1S.

Synthesis of K₂L(dme)₄:

K₂L (130 mg, 0.258 mmol) was recrystallized from cold 1,2-dimethoxyethane (dme, 5 mL). The supernatant was decanted from the yellow crystals, which were washed with cold dme (2 x 2 mL) and pentane (3 x 2 mL). Drying *in vacuo* yielded yellow K₂L(dme)₄ (110 mg, 0.127 mmol, 49%), which is insoluble in C₆D₆.

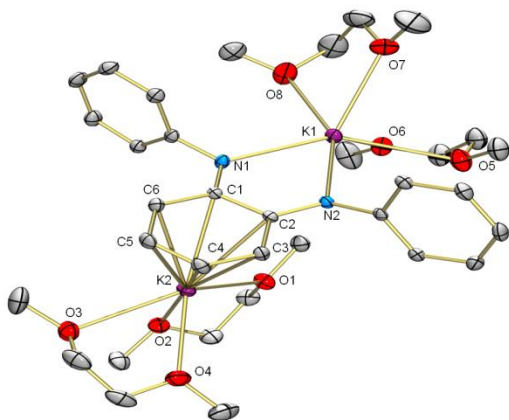


Figure S28 Molecular structure of K₂L(dme)₄ with 30% probability ellipsoids. Isopropyl groups and hydrogen atoms omitted for clarity. Selected bond lengths (\AA) and angles ($^\circ$): C1-C2 1.462(3), C2-C3 1.412(3), C3-C4 1.410(3), C4-C5 1.371(4), C5-C6 1.413(3), C1-N1 1.362(3), C2-N2 1.362(3), K1-N1 2.719(2), K1-N2 2.713(2), K1-O5 2.974(2), K1-O6 2.787(2), K1-O7 2.879(3), K1-O8 2.850(2), K2-C1 3.077(2), K2-C2 3.231(2), K2-C3 3.204(2), K2-C4 3.168(2), K2-C5 3.101(2), K2-C6 3.021(2), K2-O1 2.743(2), K2-O2 2.880(2), K2-O3 2.858(2), K2-O4 2.670(2), N1-K1-N2 61.24(6), O5-K1-O6 57.66(6), O7-K1-O8 61.68(7), O1-K2-O2 60.04(6), O3-K2-O4 59.84(6).

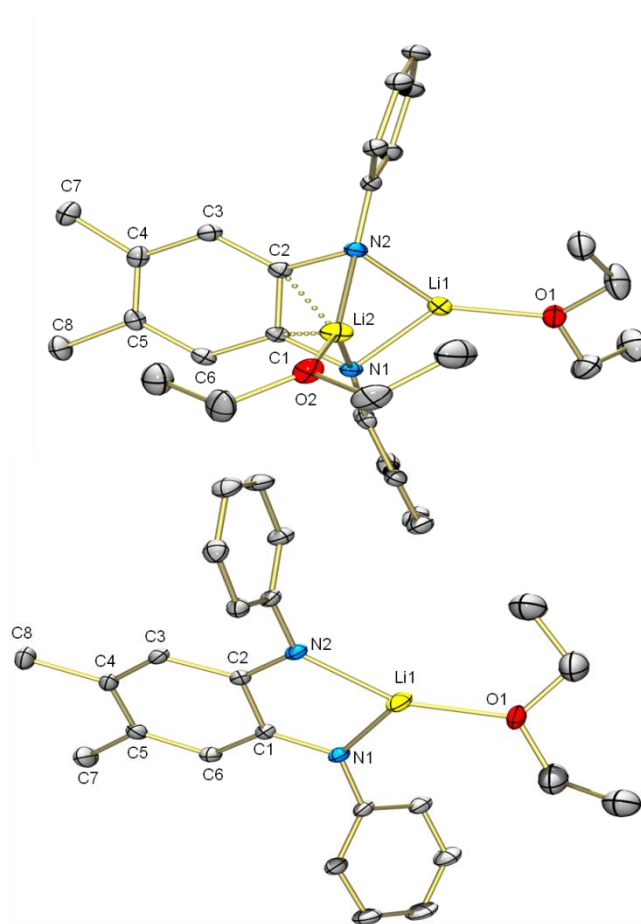


Figure S29 Molecular structures of $[\text{Li}_2\text{L}'(\text{Et}_2\text{O})_2]$, **5** (top), and $[\text{LiL}'(\text{Et}_2\text{O})]$, **6** (bottom) with 30% probability ellipsoids. Only one disordered component of Et_2O molecules is shown. Isopropyl groups and hydrogen atoms are omitted for clarity. Selected bond angles ($^\circ$) for **5**: N1-Li1-N2 85.4(1), O1-Li1-N1 129.4(2), O1-Li1-N2 141.6(2), N1-Li2-N2 80.6(1), O2-Li2-N1 134.5(2), O2-Li2-N2 144.9(2). Selected bond angles ($^\circ$) for **6**: O1-Li1-N1 118.7(2), O1-Li1-N2 153.8(3), N1-Li1-N2 87.0(1)

Table 1S Selected bond lengths in **5** and **6**

Bond	Length in 5 (\AA)	Length in 6 (\AA)	Bond	Length in 5 (\AA)	Length in 6 (\AA)
C1-C2	1.442(2)	1.464(2)	Li1-N1	1.961(3)	1.950(3)
C2-C3	1.404(3)	1.426(2)	Li1-N2	1.968(4)	1.960(3)
C3-C4	1.405(3)	1.374(2)	Li1-O1	1.871(3)	1.901(6)
C4-C5	1.404(2)	1.426(2)	Li2-N1	2.056(4)	
C5-C6	1.405(3)	1.374(2)	Li2-C1	2.291(4)	
C1-C6	1.394(2)	1.427(2)	Li2-C2	2.324(4)	
C1-N1	1.417(2)	1.337(2)	Li2-N2	2.064(4)	
C2-N2	1.407(2)	1.339(2)	Li2-O2	1.997(4)	

Discussion of the molecular structures of **5** and **6**.

Different from the solution data, the solid state structure of **5** (Figure S29) reveals that the two Li atoms occupy distinct coordination environments. Li1 resides in a distorted trigonal planar geometry: two amido nitrogen donor atoms and one oxygen from a terminal diethylether ligand occupy the three coordination sites. Li2 is tetracoordinate, engaging in an η^4 - interaction with the two diamido nitrogen donor atoms and the two N-bound *o*-phenylene carbons. The coordination sphere of Li2 is completed by a terminal diethylether ligand. The NN chelate forms longer N-Li bonds with Li2 (2.056(4) and 2.064(4) Å) than with Li1 ((1.961(3) and 1.968(4) Å). Li1 sits on one side of the C1-C2-N1-N2 plane with a dihedral angle between this plane and N1-Li1-N2 plane of 37°; Li2 sits on the other side of the C1-C2-N1-N2 plane, with a dihedral angle between this plane and N1-Li2-N2 plane of 80°. Among related dilithium complexes of *o*-phenylenediamido ligands such as **1**, the *N,N'*-disilyl versions by Lappert,⁵ or the *N,N'*-2,4,6-triisopropylphenyl version by Liddle,⁶ **5** is structurally unique in that Et₂O is used as a co-ligand instead of THF and that among these related complexes, the *ipso* carbons in **5** are bound the closest to Li (C1-Li2, 2.291(4) Å; C2-Li2, 2.324(4) Å).

The solid-state molecular structure of **6** (Figure S29) reveals that Li1 is chelated by the L⁺ ligand and is bound to a terminal disordered solvent molecule modelled as a 70/30 ratio of Et₂O/THF. The sum of the angles around Li is 359.5(4)°, consistent with a distorted trigonal planar geometry. One electron oxidation of L²⁺ led to a pronounced decrease in the respective C1-N1 and C2-N2 bond lengths to 1.337(2) and 1.339(2) Å relative to the counterparts in **5** (1.417(2) and 1.407(2) Å). Akin to the structure of [LiL(OEt₂)],⁷ elongation of the C1-C6 and C2-C3 bonds to 1.427(2) and 1.426(2) Å and compression of the C5-C6 and C3-C4 bonds each to 1.374(2) Å is also observed. In the starting diamido complex **5** these bond lengths are statistically similar.

Table 2S. Crystallographic data for **2**, **3(thf)₂**, **5**, **6**, **8**, **9**, **10**, **11**, and **K₂L(dme)₄**.

	2	3(thf)₂	5	6	8
Formula	C ₄₁ H ₆₆ ClLiN ₂ O ₂ Ta	C ₄₂ H ₆₆ LiN ₂ O ₂ Ta	C ₄₀ H ₆₂ Li ₂ N ₂ O ₂	C ₃₆ H _{51.4} LiN ₂ O	C ₃₃ H ₄₇ N ₂ Ta
FW	842.29	818.85	616.79	535.13	652.67
<i>T</i> (K)	150(2)	150(2)	150(2)	150(2)	150(2)
space group	P2 ₁ /n	Pcba	P2 ₁ /c	P2 ₁ /n	P2 ₁ /n
<i>a</i> (Å)	11.0302(4)	21.1920(16)	11.4110(15)	8.9697(4)	10.6170(19)
<i>b</i> (Å)	23.2106(8)	18.2269(12)	19.573(3)	21.8449(8)	17.966(3)
<i>c</i> (Å)	17.0382(7)	21.3088(16)	17.749(2)	17.0042(7)	16.185(3)
α (deg)	90	90	90	90	90
β (deg)	108.6064(15)	90	93.323(6)	94.395(2)	98.038(7)
γ (deg)	90	90	90	90	90
<i>V</i> (Å ³)	4134.1(3)	8230.8(10)	3957.6(9)	3322.0(2)	3056.8(9)

<i>Z</i>	4	8	4	4	4
<i>D_c</i> (g·cm ⁻³)	1.353	1.322	1.035	1.070	1.418
<i>μ</i> (mm ⁻¹)	2.757	2.705	0.061	0.063	3.618
no. of refln collected	39363	70581	19128	28427	24798
no. of indept refln	9494	9454	8876	7647	7023
GOF on <i>F</i> ²	1.183	1.150	1.010	1.040	1.128
<i>R</i> [<i>I</i> > 2σ(<i>I</i>)]	<i>R</i> ₁ = 0.0233 ^{a)}	<i>R</i> ₁ = 0.0318	<i>R</i> ₁ = 0.0579	<i>R</i> ₁ = 0.0623	<i>R</i> ₁ = 0.0290
	<i>wR</i> ₂ = 0.0577 ^{b)}	<i>wR</i> ₂ = 0.0797	<i>wR</i> ₂ = 0.1525	<i>wR</i> ₂ = 0.1718	<i>wR</i> ₂ = 0.0441
<i>R</i> (all data)	<i>R</i> ₁ = 0.0339	<i>R</i> ₁ = 0.0647	<i>R</i> ₁ = 0.1088	<i>R</i> ₁ = 0.0865	<i>R</i> ₁ = 0.0683
	<i>wR</i> ₂ = 0.0799	<i>wR</i> ₂ = 0.1160	<i>wR</i> ₂ = 0.1884	<i>wR</i> ₂ = 0.1896	<i>wR</i> ₂ = 0.0889

	9	10	11	K₂L(dme)₄
Formula	C ₄₆ H ₆₉ N ₄ Ta	C ₄₂ H ₅₈ N ₅ Ta	C ₆₄ H ₈₈ N ₄ Ta ₂	C ₄₆ H ₇₈ N ₂ O ₈ K ₂
FW	859.00	813.88	1275.28	865.30
<i>T</i> (K)	150(2)	150(2)	150(2)	149(2)
space group	P2 ₁ /n	P-1	P2 ₁ /c	P2 ₁ /n
<i>a</i> (Å)	14.1372(15)	10.4591(8)	15.9017(5)	10.8034(7)
<i>b</i> (Å)	15.1014(15)	12.8533(10)	19.5480(4)	27.6688(19)
<i>c</i> (Å)	20.108(2)	16.2426(13)	22.0555(5)	17.1421(12)
α (deg)	90	69.066(3)	90	90
β (deg)	96.647(4)	82.852(4)	92.2620(11)	98.503(2)
γ (deg)	90	76.536(3)	90	90
<i>V</i> (Å ³)	4264.1(8)	1981.3(3)	6850.5(3)	5067.7(6)
<i>Z</i>	4	2	4	4
<i>D_c</i> (g·cm ⁻³)	1.338	1.364	1.236	1.070
μ (mm ⁻¹)	2.613	2.808	3.227	0.235
no. of refln collected	37634	23806	65508	33778
no. of indept refln	9755	9050	15746	8874
GOF on <i>F</i> ²	0.956	1.040	0.933	1.039
<i>R</i> [<i>I</i> > 2 σ (<i>I</i>)]	<i>R</i> ₁ = 0.0407 ^{a)}	<i>R</i> ₁ = 0.0209	<i>R</i> ₁ = 0.0356	<i>R</i> ₁ = 0.0519
	<i>wR</i> ₂ = 0.0839 ^{b)}	<i>wR</i> ₂ = 0.0482	<i>wR</i> ₂ = 0.0791	<i>wR</i> ₂ = 0.1425
<i>R</i> (all data)	<i>R</i> ₁ = 0.0893	<i>R</i> ₁ = 0.0257	<i>R</i> ₁ = 0.0595	<i>R</i> ₁ = 0.0715
	<i>wR</i> ₂ = 0.0990	<i>wR</i> ₂ = 0.0499	<i>wR</i> ₂ = 0.0853	<i>wR</i> ₂ = 0.1600

^{a)} $R_1 = \sum(F_o - F_c)/\sum F_o$ ^{b)} $wR_2 = [\sum[w(F_o^2 - F_c^2)^2]/\sum w(F_o^2)^2]^{1/2}$

3. EPR Spectroscopy

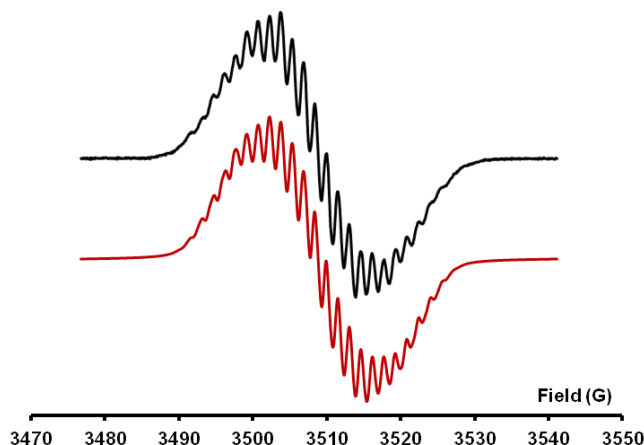


Figure S30 Experimental (top) and simulated (bottom) EPR spectrum of **6** (thf solution, room temperature) X-band microwave frequency 9.856 GHz. Parameters used in simulation: 100% Lorentzian lineshape, $g = 2.0075$, $a_N = 4.58$ G, $a_H = 3.39$ and 1.53 G, $a_{Li} = 0.85$ G,

The room temperature EPR spectrum of a THF solution of **6** is shown in Figure S30. The g factor of **6** is 2.0075; it is close to the free electron value of 2.0036, which is expected for an organic radical with negligible spin-orbit coupling. The multiplet pattern was simulated taking into account hyperfine coupling to a pair of equivalent ^{14}N nuclei, a pair of equivalent *o*-phenylene ^1H nuclei, the six equivalent 4,5-dimethyl ^1H nuclei, and one ^7Li nucleus. The multiplet pattern is consistent with delocalization of the unpaired electron throughout the *o*-phenylene framework, which has been observed in EPR spectra of $[\text{LiL}(\text{OEt}_2)]$.⁷

4. References:

1. Apex 2 Software Package; Bruker AXS Inc., Madison, WI, 2013.
2. Sheldrick, G. M. *Acta Crystallogr., Sect. A: Found. Crystallogr.* 2008, 64, 112.
3. <http://shelx.uni-ac.gwdg.de/SHELX/index.php> (accessed July 4, 2013 and September 4, 2015).
4. Spek, A. L. *J. Appl. Crystallogr.* 2003, 36, 7.
5. S. Daniele, C. Drost, B. Gehrhus, S. M. Hawkins, P. B. Hitchcock, M. F. Lappert, P. G. Merle and S. G. Bott, *J. Chem. Soc., Dalton Trans.*, 2001, 3179.
6. S. Robinson, E. S. Davies, W. Lewis, A. J. Blake and S. T. Liddle, *Dalton Trans.*, 2014, **43**, 4351-4360
7. T. Janes, J. M. Rawson and D. Song, *Dalton Trans.*, 2013, **42**, 10640-10648.